Author(s): Singh, Deepak & Martin, Floran & Rasilo, Paavo & Belachen, Anouar

Title: Magneto-Mechanical Model for Hysteresis in Electrical Steel Sheet

Year: 2016

Version: Post print

Please cite the original version:

Singh, Deepak & Martin, Floran & Rasilo, Paavo & Belachen, Anouar. 2016. Magneto-Mechanical Model for Hysteresis in Electrical Steel Sheet. IEEE Transactions on Magnetics. 9. 0018-9464 (electronic).

Magneto-Mechanical Model for Hysteresis in Electrical Steel Sheet

Deepak Singh[1], Floran Martin[1], Paavo Rasilo[1,2] and Anouar Belachen[1]
[1] Aalto University, Deprtment of Electrical Engineering and Automation, P.O. Box 13000 FI-00076 Aalto, Finland
[2]Tampere University of Technology, Department of Electrical Engineering, P.O. Box 692, FI-33101 Tampere, Finland

A coupled magneto-mechanical model for hysteresis in an electrical steel sheet is presented. The foundation of the model developed is the classical Sablik-Jiles-Atherton (SJA) model. A comprehensive model for the stress dependent magnetostriction is also proposed and implemented in the SJA model. Improvements in the SJA model as well, are proposed and validated with simultaneous measurements of magnetostriction, magnetic field and flux density. The measurements were performed on a single electrical steel sheet under various levels of stress (-35 MPa to 100 MPa). The proposed model was found to adequately model the permeability change and the local bowing of the BH-loop due to stress.

***Index Terms*—Electrical Steel, Hysteresis, Jiles-Atherton model, Magnetostriction, Magnetization and Stress**

I. Introduction

PROPERTIES of magnetic materials depend strongly on the stress state of the material. The deformation and deviation in the BH-loop of an electrical steel sheet due to stress are evident from various previous studies [1]–[3]. These effects of stress on the material properties, especially on the BH characteristic [4], [5], the iron losses [3], [6], [7] and the vibration [8], [9], are detrimental for an electrical machine [10]–[12]. In order to accound for these effects, a comprehensive magnetic and mechanics coupled (*i.e.* magneto-mechanical) model is required during the design process of electrical machines. Recent studies based on the multi-scale approach [10], [13], [14] and the thermodynamics approach [8], [15] are relevant effort to tackle the coupled problem. However, these coupled models are anhysteretic and do not account for the localized bowing of the BH-loop observed during measurements (Fig. 2 of [3]).

The model for magnetic hysteresis presented in [16], [17] is based on the principle of the magnetic domain theory and the domain wall pinning. This phenomenological model is popularly known as the Jiles-Atherton (JA) model. The JA model for magnetic hysteresis is simple and popular amongst the research community [9], [18]–[20]. Mechanical phenomena such as magnetostriction can be correlated to the magnetic phenomena using the JA model in order to study the effect of stress on the magnetic behavior of a magnetic material [21]–[23]. Based on both the thermodynamics and mechanical equilibriums, Sablik et al. [23] account for this stress effect with an additional term in the expression of the effective field. Their model, refered as the Sablik-JA (SJA) model, describes a symmetrical magnetic behavior with respect to zero stress.

Furthermore, in [24], [25] the unsymmetrical behavior of the BH-loop at tensile and compressive stress was modeled as the demagnetizing effect due to compression. Another additional term, proportional to the magnetization whose coefficient tends to zero for the tensile stress, was added to the effective field. Nevertheless, measurements in NO Fe-Si single steel sheets under alternative flux density and coaxial applied stress from -35 MPa until 100 MPa demonstrates two phenomena [3], [20]. First is a slight improvement in the permeability at small tensile stresses and the second is the local bowing of the BH loop for high compressive stress and low value of the magnetization [1]. The improvements of SJA model proposed in [24], [25] are not sufficient to model these phenomena.

In this study, the correlation between asymmetrical variation of the magnetostriction and the BH characteristic with applied coaxial stress has been explored. Based on simultaneous measurements of the magnetostriction, the magnetic field and the flux density in single NO steel sheet under various levels of compressive and tensile elastic stresses, we proposed some semi-analytical improvements of the SJA model in order to accurately represent both the effect of stress and the bowing of the BH loops. The measured magnetostriction is represented with a function of both the magnetization and the stress. Whereas the parameter, usually denoted k, related to the coercitive field is constant, we suggest to model this parameter with an additional term depending on both the stress and the magnetization. The implementation of our proposed improvements of the SJA model and its inversion for flux density input modeling application are detailed and discussed. Finally, the proposed model is validated by measurements and the accuracy of the model analyzed.

II. SJA Model

Based on the thermodynamic equilibrium [17], for an isotropic polycrystalline material with no pinning sites, anhysteretic magnetization M_{an} can be expressed as Langevin function of H_e/a

$$M_{an} = M_s \left(\coth\left(\frac{H_e}{a}\right) - \frac{a}{H_e} \right) \tag{1}$$

$$H_e = H + \alpha M \tag{2}$$

where M_s, M, $H$and H_e are the saturation magnetization, total magnetization, applied magnetic field and effective magnetic

Manuscript received January 28, 2016; revised Xxxx xx, xxxx; accepted Xxxx xx, xxxx. Date of publication Xxxx xx, xxxx; date of current version Xxxx xx, xxxx. Corresponding author: D. Singh (email: deepak.singh@aalto.fi). Color versions of one or more of the figures in this paper are available online at http://ieeexplore.ieee.org. Digital Object Identifier (inserted by IEEE).

field respectively. The parameter α is a dimensionless mean field parameter representing interdomain coupling and a is the anhysteretic form factor. The total magnetization M is the sum of the reversible part M_{rev} owing to the bending of the domain walls and the irreversible part M_{irr} representing the domain wall translation. Furthermore, both the irreversible and the reversible magnetization could be expressed in terms of deviation of M_{irr} from M_{an},

$$M = M_{rev} + M_{irr} \tag{3}$$

$$M_{rev} = c\left(M_{an} - M_{irr}\right) \tag{4}$$

$$M = (1-c)M_{irr} + cM_{an} \tag{5}$$

$$\frac{dM_{irr}}{dH_e} = \frac{M_{an} - M_{irr}}{k\delta} \tag{6}$$

$$\delta = \begin{cases} +1 & \text{if } \dfrac{dH}{dt} \geq 0 \\ -1 & \text{if } \dfrac{dH}{dt} < 0 \end{cases}$$

$$B = \mu_0\left(H + M\right) \tag{7}$$

where, B is the magnetic flux density. The JA model parameter c refers to the reversal parameter that depends on bowing of the domain wall, k is the wall pining parameter which defines the coercive field H_c and μ_0 is the permeability of the vacuum. The sign of dH/dt, denoted δ, produces the hysteresis by ensuring the opposition between the domain-wall pinning and the magnetization [23]. Hence, the magnetic field is always leading the magnetic flux density.

The effect of stress is modeled as an additional term in the effective field H_e [23],

$$H_e = H + \alpha M + H_\sigma \tag{8}$$

where H_σ is the stress contribution on the effective field. According to [23] sign of H_σ must change with sign of the magnetization, as the movement of domains due to the applied stress can only assist (oppose) in the direction of magnetization. Furthermore, magnetization causes the domains of a magnetic material to be oriented in the magnetization direction. The rearrangement of the domains elongates or retracts the specimen in the orientation parallel to the magnetization. This phenomenon, also termed *magnetostriction*, deforms the specimen with volume conservation [26], it involves strain in other orthogonal orientations. In this article, the term magnetostriction refers to the deformation along the magnetization direction. Moreover, the magnetostriction λ is an even function of the magnetization (*i.e.* deformation due to the magnetization is independent of its direction). Since the applied stress can as well affect the domain structure due to magnetoelastic interaction, all the three magneto-mechanical quantities (*i.e.* λ, M and σ) are interrelated. Originally, the stress contribution on the effective field was developed in a phenomenological manner in [23]. Sablik et al. improved its expression in [27], based on thermodynamic equilibrium. For ideal polycrystals, this field related to stress can be modeled by

$$H_\sigma = \frac{3}{2}\frac{\sigma}{\mu_0}\left(\frac{\partial\lambda}{\partial M}\right)_\sigma. \tag{9}$$

III. Proposed Magneto-Mechanical Model

A. Magnetostriction Model

As mentioned earlier, the magnetostriction is an even function of the magnetization. Additionally, the magnetostriction also depends on the applied coaxial stress. Various previous studies have either used ad-hoc function or linear dependency of the magnetostriction λ with respect to compressive and tensile stresses [27], [28]. However, some publications based on the measurements clearly show the nonuniform dependency of λ on the compressive and the tensile stress with coaxial σ and M [29]–[31]. The model for λ proposed here is the product of two distinct functions (*i.e.*function of magnetization M and function of stress σ),

$$\lambda = \left(\sum_{j=1}^{p} a_j M^{2j}\right) b_1\left(b_2 + \tanh\left(\frac{b_3 - \sigma}{b_4}\right)\right) \tag{10}$$

$$\lambda = f(M)g(\sigma). \tag{11}$$

The first function in (11), $f(M)$ is an even function of magnetization M and has been extensively used in previous studies relating magnetostriction with the JA model (both hysteretic and anhysteretic models) [21], [23], [32]. Furthermore, in the previous studies coefficients of the even polynomial function $f(M)$ were made stress dependent, albeit symmetrical with respect to the compressive and the tensile stress. The second function in (11), $g(\sigma)$ scales $f(M)$ depending on the stress σ and this scaling is asymmetrical with respect to stress. The parameters b_3 and b_4 control the shift and slope of the hyperbolic tangent function with respect to σ, respectively. The argument of $\tanh$ contains $-\sigma$, which implies that it is flipped with respect to the stress (compression being negative and tension positive on the stress axis). This is evident from Figure (12a) of [30], which shows the variation of the maximum magnetostriction with respect to stress.

B. Improved SJA Model

The expression for H_σ was originally derived from the thermodynamics equilibrium assuming perfect crystalline structure of the material. Due to the manufacturing process of electrical steel sheets, the domains and their walls should not be considered as ideal. To account for this fact, a stress factor γ_σ termed as *magnetostriction coupling factor* is introduced in the expression for H_σ. Moreover, the effect of H_σ diminishes at the magnetization level close to saturation (as observed during measurements, Fig. 7). Which implies,

$$H_\sigma = \begin{cases} \dfrac{3}{2}\gamma_\sigma\dfrac{\sigma}{\mu_0}\left(\dfrac{\partial f(M)}{\partial M}\right)g(\sigma) & M \leq M_{\text{hi}} \\ 0 & M > M_{\text{hi}} \end{cases} \tag{12}$$

where M_{hi} is the magnetization value at (or close to) the peak magnetostriction λ_{pk}.

Furthermore, to account for the bowing of the BH-loop (Fig. 7) at high compressive stress and low induction level, the parameter k is made M dependent,

$$k_\sigma = k + k_1 \exp\left(\frac{-\left(M+\delta m_0\right)^2}{2\beta^2}\right) \qquad (13)$$
$$k_1 \approx 0 \quad \text{if } \sigma \geq 0$$

where the parameters m_0 represents the magnetization level at which the peak bowing in the BH-loop occurs and β is the magnetization interval either side of m_0 where the bowing in the BH-loop persist. Because such a bowing is not observed when at tension, $k_1 \approx 0$. Similar approach of field or flux dependency of the parameter k has been reported in [33]–[35], albeit for better fitting of the JA-model.

IV. Model Implementation

Following are the successive steps in the implementation of the SJA model:

A. Estimation of M_{an}:

The expression of M_{an}, for the NO electrical steel has inherent error when fitting the parameters of the Langevin approximation. This error overshadows the slight variation observed in BH-loop at low tensile stresses. In-order to circumvent this problem, the anhysteretic magnetization is modeled with a cubic spline interpolation of the effective field H_e without mechanical stress. The values of M and H from previous time step is used to determine the stress contribution H_σ and the effective field H_e to be used in the interpolation for M_{an},

$$[H_\sigma]^n = \frac{3}{2}\gamma_\sigma \frac{\sigma}{\mu_0}\left[\frac{\partial \lambda}{\partial M}\right]^n \qquad (14)$$

$$[H_e]^{n+1} = [H]^n + \alpha\,[M]^n + [H_\sigma]^n \qquad (15)$$
$$[M_{an}]^{n+1} = F_0\left([H_e]^{n+1}\right) \qquad (16)$$

where F_0 is the interpolation function and n is the step number of discretized B . The step size ΔB should be small enough such that $[H_e]^{n+1} \simeq [H_e]^n$.

B. Computation of dM_{an}/dH_e, dM_{irr}/dH_e and dM/dH_e:

Once again the values of M from previous time step and the estimated M_{an} are injected in (5) and (6). The incremental terms dM_{an}/dH_e, $dM_{irr}/dH_e$and dM/dH_e are computed as

$$\left[\frac{dM_{an}}{dH_e}\right]^{n+1} = F_0'\left([H_e]^{n+1}\right) \qquad (17)$$

$$[M_{irr}]^{n+1} = \frac{[M]^n - c\,[M_{an}]^{n+1}}{1-c} \qquad (18)$$

$$\left[\frac{dM_{irr}}{dH_e}\right]^{n+1} = \frac{[M_{an}]^{n+1} - [M_{irr}]^{n+1}}{k_\sigma \delta} \qquad (19)$$

$$\left[\frac{dM}{dH_e}\right]^{n+1} = (1-c)\,\delta_m\left[\frac{dM_{irr}}{dH_e}\right]^{n+1} + c\left[\frac{dM_{an}}{dH_e}\right]^{n+1} \qquad (20)$$

$$\delta_m = \begin{cases} 0 & \text{if } \dfrac{dH}{dt} < 0 \;\&\; M_{an}(H_e) \geq M(H) \\ 0 & \text{if } \dfrac{dH}{dt} \geq 0 \;\&\; M_{an}(H_e) \leq M(H) \\ 1 & \text{otherwise} \end{cases}$$

where δ_m is the parameter to avoid unphysical behavior (*i.e.* negative susceptibilities) at the tip of the BH-loop [36].

C. Computation of dM/dH:

After some mathematical operation and substitution utilizing (14) through (20), the required expressions for the differential susceptibility (*i.e.* dM/dH) is expressed as,

$$\left[\frac{dM}{dH}\right]^{n+1} = \frac{\left[\dfrac{dM}{dH_e}\right]^{n+1}}{1-\left(\alpha + \dfrac{3}{2}\gamma_\sigma \dfrac{\sigma}{\mu_0}\left[\dfrac{\partial^2 \lambda}{\partial M^2}\right]^n\right)\left[\dfrac{dM}{dH_e}\right]^{n+1}}. \qquad (21)$$

D. Computation of M and H:

Finally, the values of M and H for the current time step are obtained as following,

$$\left[\frac{dM}{dB}\right]^{n+1} = \frac{\left[\dfrac{dM}{dH}\right]^{n+1}}{\mu_0\left(1+\left[\dfrac{dM}{dH}\right]^{n+1}\right)} \qquad (22)$$

$$[M]^{n+1} = [M]^n + \Delta B\left[\frac{dM}{dB}\right]^{n+1} \qquad (23)$$

$$[H]^{n+1} = \frac{1}{\mu_0}[B]^{n+1} - [M]^{n+1}. \qquad (24)$$

This solution method for inverting the SJA model is summarized in the flow chart of Fig. 1.

V. Measurement Setup

Fig. 2 shows the magnetization core and the single sheet tester (SST) sample along with the custom-built stressing device having a range and resolution of ± 1250 N and 1 N, respectively. A programmable power source and a data acquisition system (DAQ) with analog output were used in conjunction with a PC to control the magnitude and waveform of the supply voltage so as to produce a sinusoidal induction in the SST sample. The feedback control of the supply voltage was programmed using MATLAB/DAQ toolbox. In addition to that, a high speed DAQ system and low-noise/high-gain signal amplifiers were used to retrieve the measured signals for the field strength and the flux density. Tunneling magnetoresistance (TMR) sensors arranged in a 2×2 grid were used

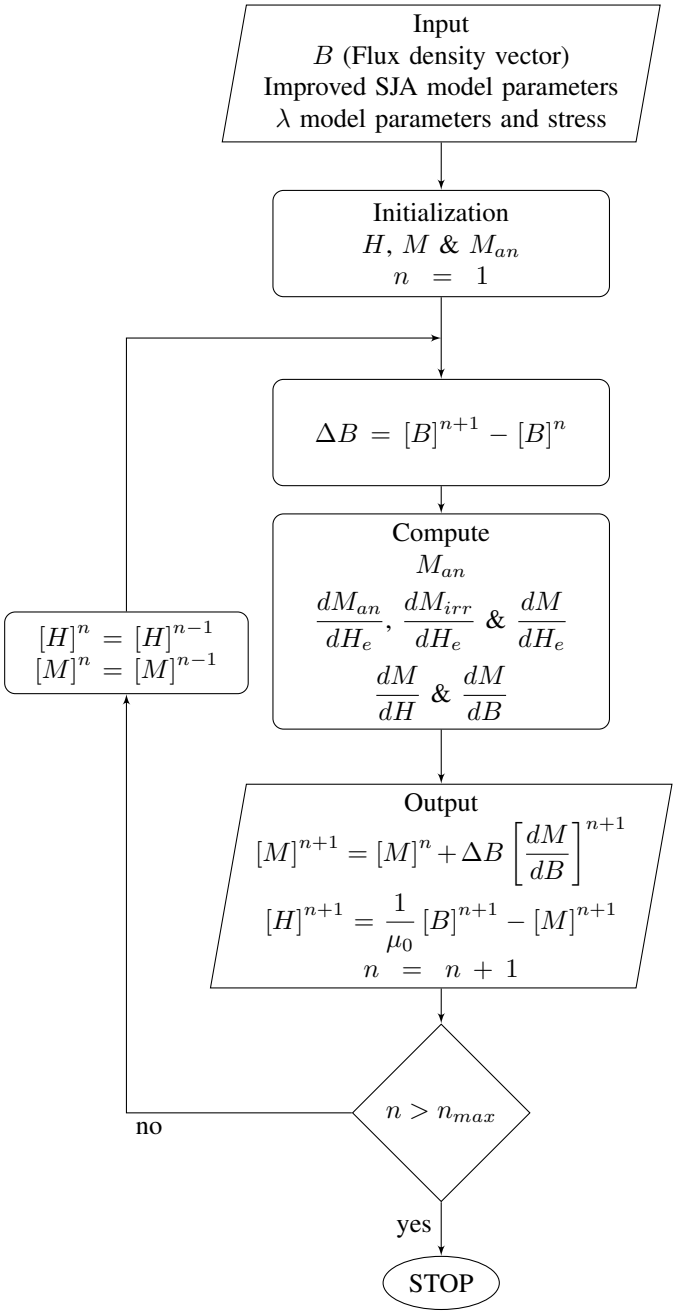

Fig. 1. Flow chart for the solution method of the SJA model

to measure the surface magnetic field strength, and a coil wound around the sample was used to measure the magnetic flux density. Furthermore, a non-inductive type of strain gauge rosette (H-series rosette from Micro-Measurements), glued on the surface of the sample (with the insulating coating removed) was used to measure the magnetostriction. Fig. 3 shows the SST sample and placement of the magnetic field sensors, the strain rosette and the search coil on the sample. The SST sample shown in Fig. 3 was made along the rolling direction (RD) of 0.5 mm thick sheet of 5% Fe-Si using a milling cutter.

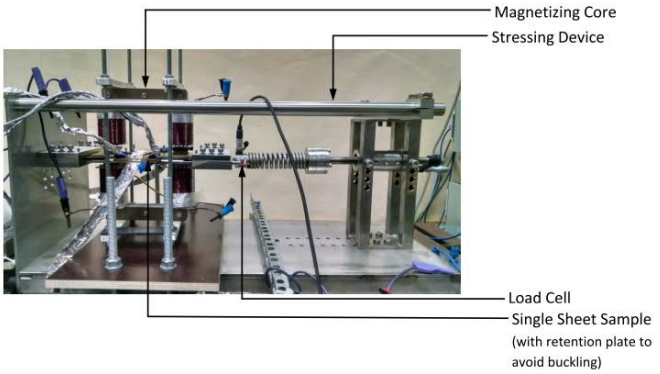

Fig. 2. Measurement setup for unidirectional magnetization and co-linear stress

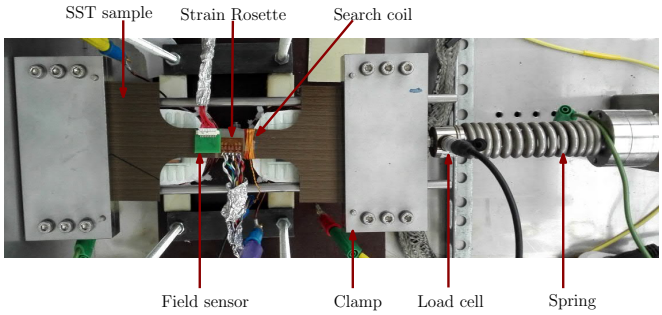

Fig. 3. Unidirectional SST sample with sensor and coil positioning.

VI. Result and Discussion

A. Fitting the improved SJA model parameters

There are three distinct steps to be followed during the fitting of the coupled magneto-mechanical model parameters.

1) Step 1: Fitting SJA parameters without stress

First, the parameters of the SJA and the cubic spline interpolation of the anhystretic curve are fitted from the BH loop without stress, implying $H_\sigma = 0$. The starting values of the JA model parameter can be obtained from the initial and the maximum magnetic susceptibility of the first magnetization curve and the magnetic susceptibility at the points of the remanent flux density B_r and the coercive field H_c [36].

2) Step 2: Fitting magnetostriction model

Both the polynomial coefficient a_j and the parameters of $g(\sigma)$ of the proposed magnetostriction expression (10) are fitted with the magnetostriction measurements.

3) Step 3: Fitting remaining stress dependent parameters

With the parameters previously determined, the parameters of the Gaussian function in (13) are extracted by fitting k_σ, γ_σ, m_0 and β for every level of stress. Since the values of m_0 and β were found constants, they are considered independent from stress.

The *least square error estimation* subroutine LSQCURVEFIT of MATLAB was used for the curve fitting during this study. Furthermore, as the SJA model inherently starts from origin (*i.e.* $B \approx 0$ and $H \approx 0$), for step 1 and 3 two cycles of the flux density waveform were simulated and the last cycle was used for the fitting against the measured B and H.

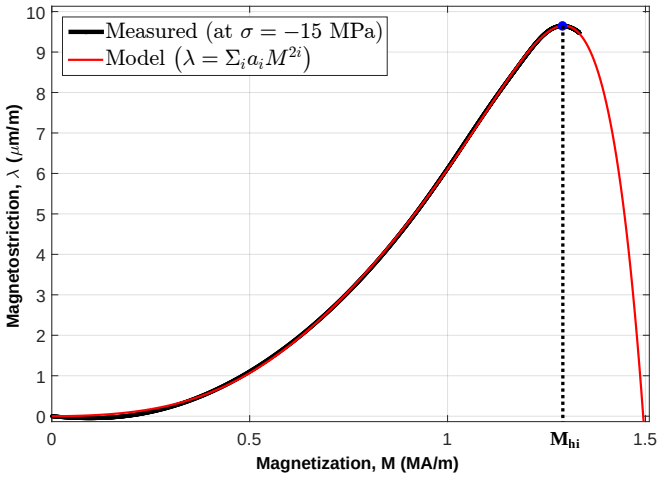

Fig. 4. Measured and fitted λ v/s M. M_{hi} is the magnetization level at which the slope of λM-curve changes sign *i.e.* $d\lambda/dM = 0$. This change is also observed during measurement.

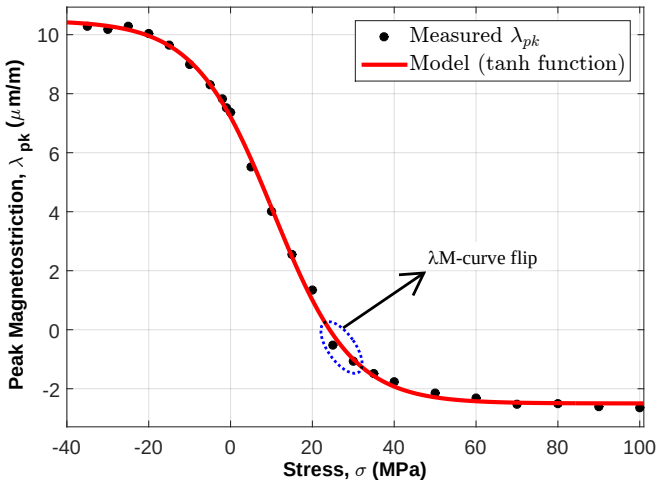

Fig. 5. Measured and fitted peak magnetostriction λ_{pk} v/s σ. The saturation of λM-curve with stress and the flip of λM-curve can be observed.

B. Magnetostriction model fitting

The measurements for this study were carried out on the SST sample cut along the rolling direction (RD). The measurements were done at the supply frequency of 6 Hz and the stress levels between -35 MPa to +100 MPa. The signals of measured quantities were acquired at the sampling frequency of 50 kHz. Furthermore, the measured magnetostriction was averaged over 10 cycles. The estimation of coefficients for the function $f(M)$ were done using the measurement at $\sigma = -15$ MPa (Fig. 4). Similarly, peak values of the measured magnetostriction at every stress levels were used to determine the coefficients of the function $g(\sigma)$ (Fig. 5). Fig. 6 shows the measured and the modeled λ and Table I contains the parameters of the stress dependent magnetostriction model. Measured magnetostriction at any stress level can be used to fit the polynomial coefficient a_j, although with appropriate scaling b_1. Magnetostriction measured at $\sigma = -15$ MPa was used for better accuracy. Previous stress dependent λM models had the coefficients a_j as the polynomial of stress [32] and the coefficients had to be fitted all at once (all stress levels at once) which led to the non-optimal solution for the fitting. Moreover, with the polynomial of σ it is not possible to model the trend observed in Fig. 5.

TABLE I. Values of parameters of magnetostriction model

Parameter	Value	Parameter	Value
a_1	2.085×10^{-18}	b_1	0.6729
a_2	11.96×10^{-30}	b_2	0.6151 μm/m
a_3	-15.17×10^{-42}	b_3	10.44 MPa
a_4	9.683×10^{-54}	b_4	19.21 MPa
a_5	-2.452×10^{-66}		

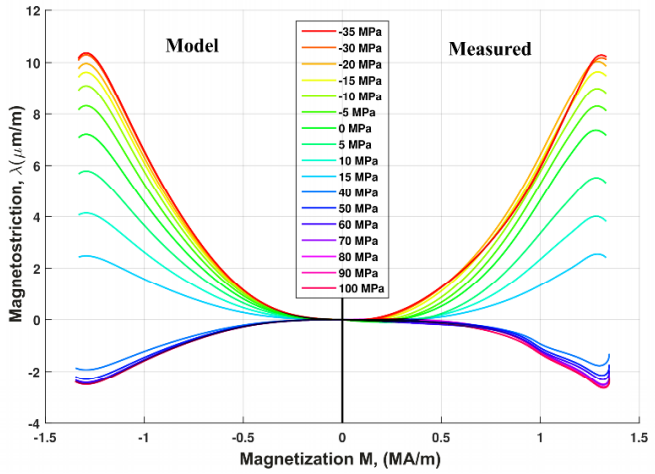

Fig. 6. Measured and modeled stress dependent λ

From the measurements, the asymmetrical behavior of the λM-curve with stress is evident. Most interesting is the fact that the λM-curve flip (Fig. 5) around the abscissa axis and almost simultaneously the deterioration of the permeability occurs for tensile stress level between 25 to 30 MPa. Which implies that the H_σ is positive only for small tensile stress, hence the slight improvement in permeability (Fig. 9).

C. Model Comparison

The stress independent parameters of the model *i.e.* k_1, α, c, b_0 and β, obtained using the steps explained in Section IV, are presented in Table II. The value for M_{hi}, which is the magnetization amplitude at or close to the peak magnetostriction (*i.e.* $\partial\lambda/\partial M = 0$), is determined using the modeled λM-curve (Fig. 4).

TABLE II. Values of SJA model parameters

Parameter	Value
k_1	41.53 A/m
α	6.5904×10^{-6}
c	0.0001
m_0	$0.3/\mu_0$ A/m
β	$0.125/\mu_0$ A/m
M_{hi}	1.3×10^{6} A/m

Figures 7-10 show the result of the model fitting. Furthermore, sub-figures (a) and (b) of the Figures 7-10 present

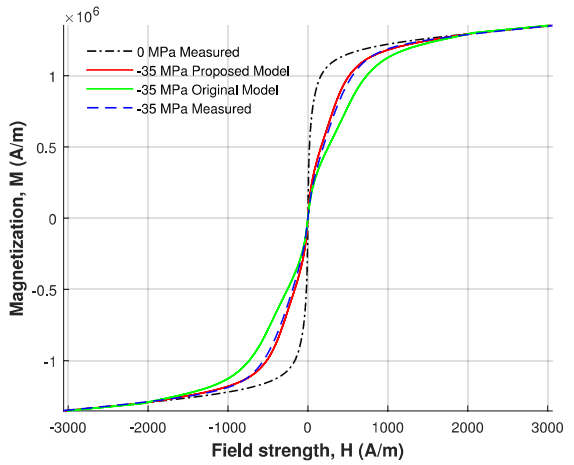

(a) M_{an} v/s H

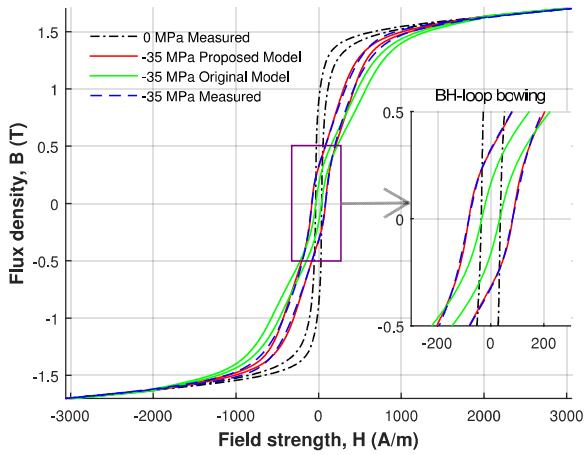

(b) BH loop

Fig. 7. Measured and modeled (a) Anhysteretic magnetization curve and (b) BH-loop at $\sigma = -35$ MPa. Overestimation of H_σ by the original SJA-model and the non-existence of the stress effect at high magnetization (saturation) can be observed. Error of the original SJA-model in modeling bowing can also be seen in sub-figure (b).

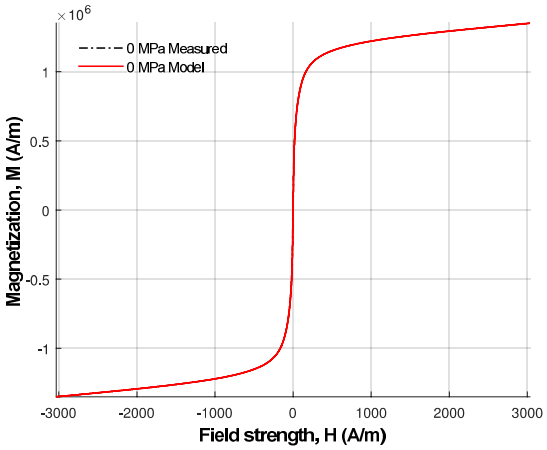

(a) M_{an} v/s H

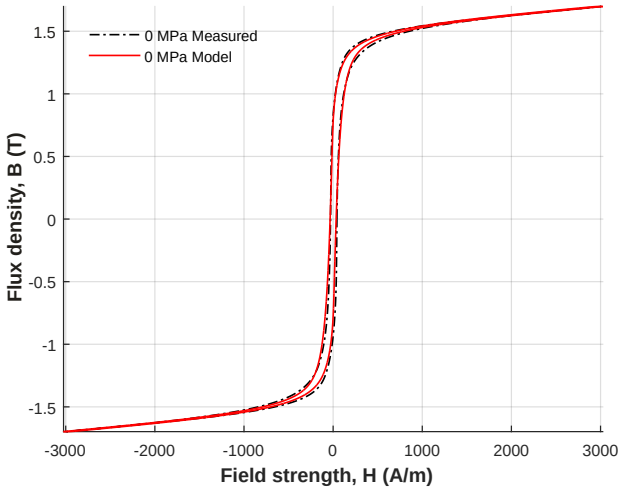

(b) BH loop

Fig. 8. Measured and modeled (a) Anhysteretic magnetization curve and (b) BH-loop at $\sigma = 0$ MPa. Both the proposed model and the original SJA-model are same for $\sigma = 0$, thus has been plotted as one model.

the anhysteretic MH-curve and the BH-loop at various stress levels, respectively. All the figures contain the measured values at zero MPa as a reference. The original SJA-model with parameter $\gamma_\sigma = 1$ is not able to reproduce correctly the anhysteretic curves for high value of compression (Fig. 7a) and tensile stress (Fig. 10a), it would be employ with small error for low tensile stress with this material (Fig. 9a). Moreover, this model does not reproduce the local enlarging of the B-H loop under compression (Fig. 7b). The measured curves in Fig. 7 and 10 show that at saturation (*i.e.* high value of magnetization) stress do not effect the MH-curve, which justifies the condition $H_\sigma = 0$ at $M > M_{hi}$ used in (12). Furthermore, the modeled results are in good agreement with the measurements, especially for the compression and lower values of the tensile stress. The error of the model fitting at higher levels of the tensile stress can be attributed to two sources. First one, is due to the error associated with the basic JA-model parameters fitting (Fig. 8) and second is the error in modeling λM-curve (after the flip about $\lambda = 0$ axis). Particularly, the initial slope of λM-curve and the magnetization level at which the peak magnetostriction λ_{pk} occur *i.e.* M_{hi}, are the major source of error, which in turn causes error at the knee of the anhysteretic curve (Fig. 10a). Thus, a separate set of parameters a_j after the λM-curve flip could be used to improve the accuracy of the model at the high tensile stresses. Furthermore, bowing of the BH-loop at high compression and low field could be phenomenologically interpreted as either the thickening of the domain walls, or the growth of 90° domains (*i.e.* orthogonal to the stress direction) which in turns encompasses more number of impurities sites.

Figures 11 and 12 show the variation of the parameters k_1 and γ_σ with stress, respectively. The variation of the parameter k_1 correlates with the measurements. As no bowing of the BH-loop at low induction (B) is observed for $\sigma \geq 0$ MPa, hence $k_1 \approx 0$. Similarly, as shown in Fig. 12, during the stress levels where $H_\sigma = 0$, *i.e.* either $\sigma \approx 0$ or $\partial\lambda/\partial M \approx 0$, the parameter γ_σ dose not have any significance. Furthermore, from Fig. 13 and Fig. 14, it is abundantly clear that the parameter k_σ influences H_c and losses. In the modified model, because $k_\sigma \approx k$ for $\sigma \geq 0$, an extra stress dependent term that is non zero for the tensile stresses and independent of M (unlike k_1) can

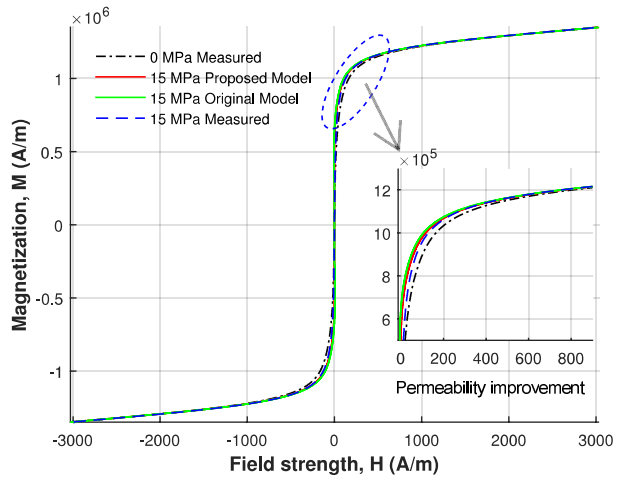

(a) M_{an} v/s H

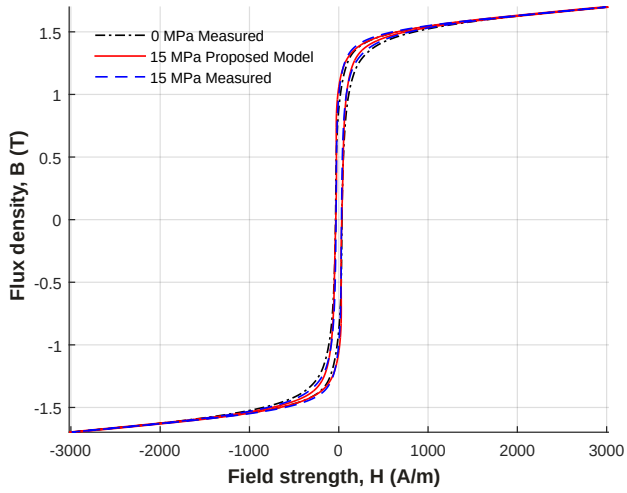

(b) BH loop

Fig. 9. Measured and modeled (a) Anhysteretic magnetization curve and (b) BH-loop at $\sigma = 15$ MPa. Overestimation of H_σ by the original model can be seen, however not distinct. As the error in MH-curve is not distinct and $k_1 = 0$ for tension, the plot of BH-loop from the original model becomes irrelevant.

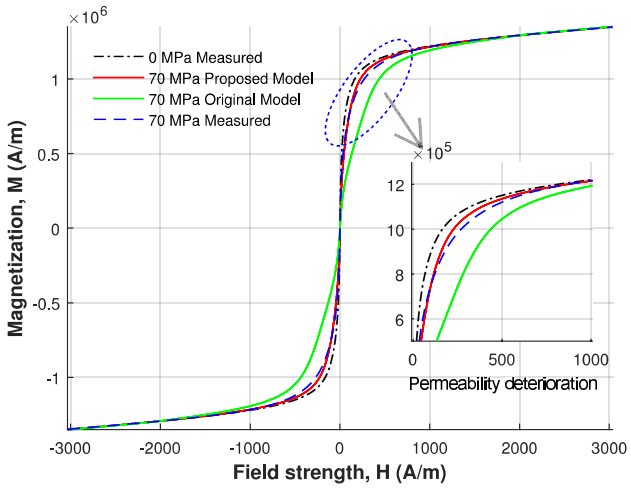

(a) M_{an} v/s H

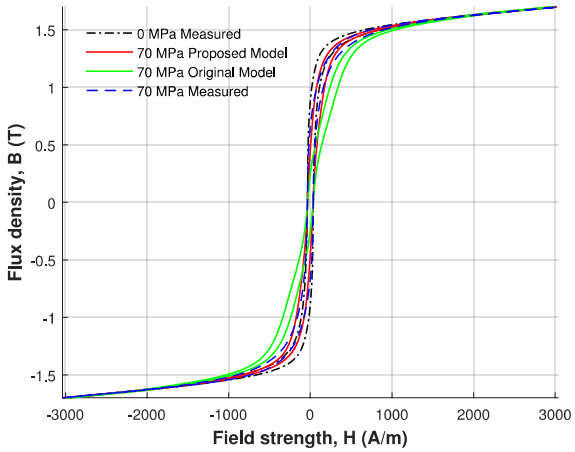

(b) BH loop

Fig. 10. Measured and modeled (a) Anhysteretic magnetization curve and (b) BH-loop at $\sigma = 70$ MPa. Overestimation of H_σ by the original SJA-model and the non-existence of the stress effect at high magnetization (saturation) can be observed.

be used in (13) for better modeling H_c at tension. Similarly from Fig. 15, it is apparent that the utilization of parameter γ_σ for fitting the anhysteretic magnetization (MH-curve) also improves the estimation of the differential permeability μ_{diff}. However, it is obvious that using $\gamma_\sigma = 1$ (as in conventional SJA Model) overestimates the stress contribution H_σ term in the effective field H_e, as shown in Fig. 7a and Fig. 10a.

VII. Conclusion

The stress dependent SJA model and its implementation method were extensively discussed. A comprehensive model for the stress dependent magnetostriction was proposed based on the measurement results. The proposed magnetostriction model was used in conjunction with the SJA model to illustrate the effect of stress on the BH-loop of a NO sheet of 0.5 mm thickness and 5% Fe-Si. Modifications in the stress induced field and the parameter k of the SJA model were also proposed. Finally, the model was fitted against the simultaneously measured λ, B and H (along the rolling direction) at various

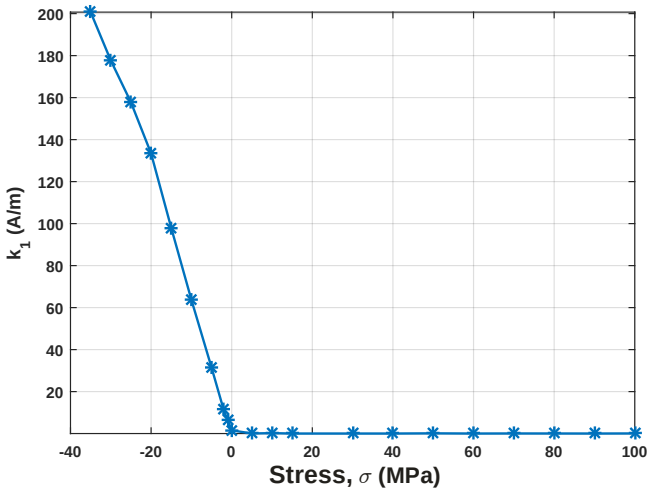

Fig. 11. Variation of parameter k_1 with respect to stress

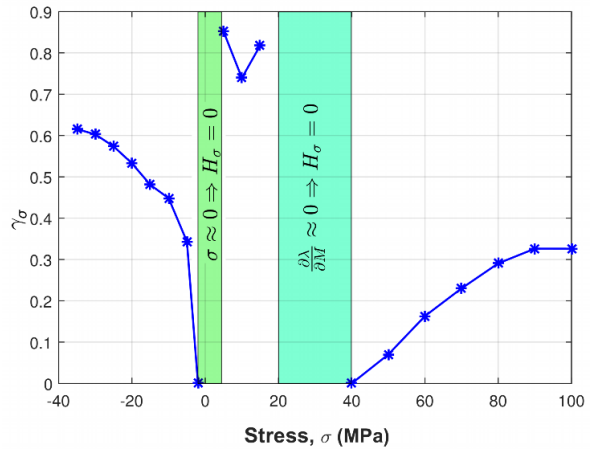

Fig. 12. Variation of parameter γ_σ with respect to stress. Highlighted are the stress values where γ_σ is of no significance.

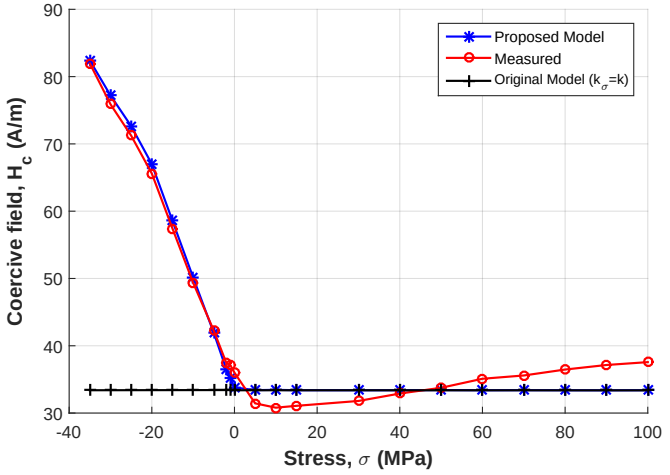

Fig. 13. Modeled and measured coercive field with respect to stress. Figure also shows the model without modification of k, *i.e.* $k_\sigma = k$.

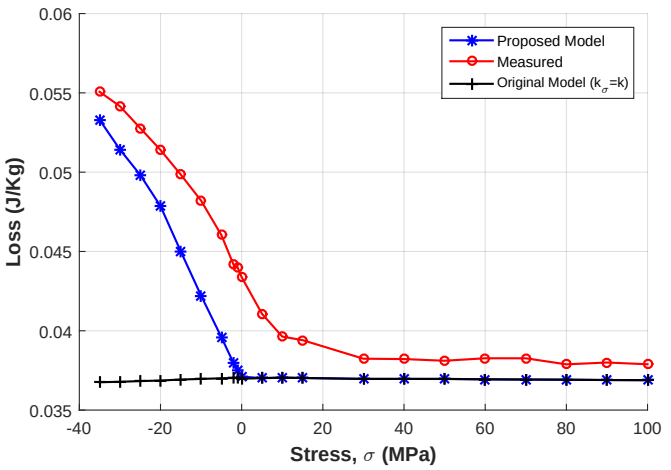

Fig. 14. Modeled and measured hysteresis loss at peak induction of 1.5 T with respect to stress. Figure also shows loss from the model without modification of k, *i.e.* $k_\sigma = k$.

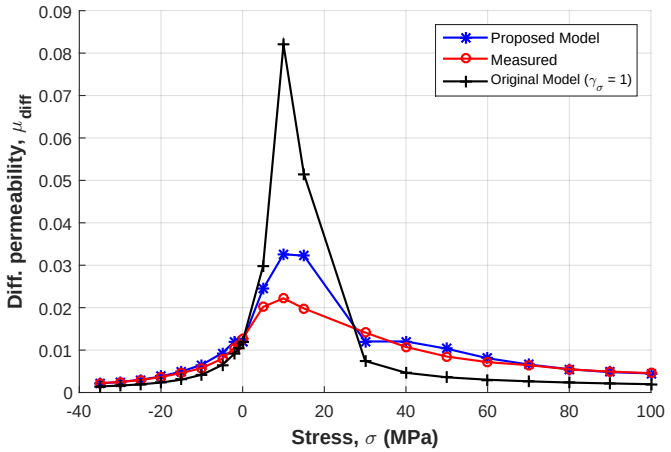

Fig. 15. Modeled and measured differential permeability μ_{diff} at 0.7 T with respect to stress. Figure also shows μ_{diff} from the model without modification in H_σ, *i.e.* $\gamma_\sigma = 1$.

compressive and tensile stress levels. The co-relation between the asymmetrical variation in the λM-curve and the BH characteristic with respect to the compression and tension stress, were analyzed. As per the results discussed in the section above, it can be concluded that the proposed model was in good agreement with the measured results. Measurements in directions other then RD and on other grade of electrical steel sheet (3% Fe-Si, 0.5 mm) have been planned for future studies, along with the first reversal and the minor-loop modeling.

Acknowledgment

The research leading to these results has received funding from the European Research Council under the European Union's Seventh Framework Programme (FP7/2007-2013) / ERC grant agreement n°339380. The authors thank the Finnish Foundation for Technology Promotion (TES), CLEEN Ltd. and Academy of Finland for their financial support.

References

[1] M. LoBue, C. Sasso, V. Basso, F. Fiorillo, and G. Bertotti, "Power losses and magnetization process in fesi non-oriented steels under tensile and compressive stress," *Journal of Magnetism and Magnetic Materials*, vol. 215216, no. 0, pp. 124–126, 2000.

[2] D. Miyagi, K. Miki, M. Nakano, and N. Takahashi, "Influence of compressive stress on magnetic properties of laminated electrical steel sheets," *IEEE Transactions on Magnetics*, vol. 46, no. 2, pp. 318–321, 2010.

[3] D. Singh, P. Rasilo, F. Martin, A. Belahcen, and A. Arkkio, "Effect of mechanical stress on excess loss of electrical steel sheets," *IEEE Transactions on Magnetics*, vol. 51, no. 11, pp. 1–4, 2015.

[4] Y. Kai, Y. Tsuchida, T. Todaka, and M. Enokizono, "Influence of stress on vector magnetic property under alternating magnetic flux conditions," *IEEE Transactions on Magnetics*, vol. 47, no. 10, pp. 4344–4347, 2011.

[5] Y. Kai, Y. Tsuchida, T. Todaka, and M. Enokizono, "Influence of stress on vector magnetic property under rotating magnetic flux conditions," *IEEE Transactions on Magnetics*, vol. 48, no. 4, pp. 1421–1424, 2012.

[6] A. Moses, "Effects of stresses on magnetic properties of silicon-iron laminations," *Journal of Materials Science*, vol. 9, no. 2, pp. 217–222, 1974.

[7] M. Rekik, L. Daniel, and O. Hubert, "Equivalent stress model for magnetic hysteresis losses under biaxial loading," *IEEE Transactions on Magnetics*, vol. 50, no. 4, pp. 1–4, 2014.

[8] K. Fonteyn, A. Belahcen, R. Kouhia, P. Rasilo, and A. Arkkio, "Fem for directly coupled magneto-mechanical phenomena in electrical machines," *IEEE Transactions on Magnetics*, vol. 46, no. 8, pp. 2923–2926, 2010.

[9] L. Vandevelde, J. Gyselinck, M. De Wulf, and J. Melkebeek, "Finite-element computation of the deformation of ferromagnetic material taking into account magnetic forces and magnetostriction," *IEEE Transactions on Magnetics*, vol. 40, no. 2, pp. 565–568, 2004.

[10] L. Bernard, X. Mininger, L. Daniel, G. Krebs, F. Bouillault, and M. Gabsi, "Effect of stress on switched reluctance motors: A magneto-elastic finite-element approach based on multiscale constitutive laws," *IEEE Transactions on Magnetics*, vol. 47, no. 9, pp. 2171–2178, 2011.

[11] K. Fujisaki, R. Hirayama, T. Kawachi, S. Satou, C. Kaidou, M. Yabumoto, and T. Kubota, "Motor core iron loss analysis evaluating shrink fitting and stamping by finite-element method," *IEEE Transactions on Magnetics*, vol. 43, no. 5, pp. 1950–1954, 2007.

[12] D. Miyagi, N. Maeda, Y. Ozeki, K. Miki, and N. Takahashi, "Estimation of iron loss in motor core with shrink fitting using fem analysis," *IEEE Transactions on Magnetics*, vol. 45, no. 3, pp. 1704–1707, 2009.

[13] L. Daniel and O. Hubert, "Equivalent stress criteria for the effect of stress on magnetic behavior," *IEEE Transactions on Magnetics*, vol. 46, no. 8, pp. 3089–3092, 2010.

[14] L. Daniel, "An analytical model for the effect of multiaxial stress on the magnetic susceptibility of ferromagnetic materials," *IEEE Transactions on Magnetics*, vol. 49, no. 5, pp. 2037–2040, 2013.

[15] U. Aydin, P. Rasilo, D. Singh, A. Lehikoinen, A. Belahcen, and A. Arkkio, "Coupled magneto-mechanical analysis of iron sheets under biaxial stress," *IEEE Transactions on Magnetics*, vol. PP, no. 99, pp. 1–1, 2015.

[16] D. Jiles and D. Atherton, "Ferromagnetic hysteresis," *IEEE Transactions on Magnetics*, vol. 19, no. 5, pp. 2183–2185, 1983.

[17] D. C. Jiles and D. L. Atherton, "Theory of ferromagnetic hysteresis (invited)," *Journal of Applied Physics*, vol. 55, no. 6, 1984.

[18] J. Leite, A. Benabou, N. Sadowski, and M. da Luz, "Finite element three-phase transformer modeling taking into account a vector hysteresis model," *IEEE Transactions on Magnetics*, vol. 45, no. 3, pp. 1716–1719, 2009.

[19] P. Rasilo, D. Singh, A. Belahcen, and A. Arkkio, "Iron losses, magnetoelasticity and magnetostriction in ferromagnetic steel laminations," *IEEE Transactions on Magnetics*, vol. 49, no. 5, pp. 2041–2044, 2013.

[20] P. Rasilo, D. Singh, U. Aydin, F. Martin, R. Kouhia, A. Belahcen, and A. Arkkio, "Modeling of hysteresis losses in ferromagnetic laminations under mechanical stress," *IEEE Transactions on Magnetics*, vol. PP, no. 99, pp. 1–1, 2015.

[21] D. Jiles and D. Atherton, "Theory of the magnetisation process in ferromagnets and its application to the magnetomechanical effect," *Journal of Applied Physics*, vol. 17, no. 6, p. 1265, 1984.

[22] D. Atherton and D. Jiles, "Effects of stress on the magnetization of steel," *IEEE Transactions on Magnetics*, vol. 19, no. 5, pp. 2021–2023, 1983.

[23] M. Sablik, H. Kwun, G. Burkhardt, and D. Jiles, "Model for the effect

[23] M. Sablik, H. Kwun, G. Burkhardt, and D. Jiles, "Model for the effect of tensile and compressive stress on ferromagnetic hysteresis," *Journal of Applied Physics*, vol. 61, no. 8, pp. 3799–3801, 1987.

[24] M. Sablik, "A model for asymmetry in magnetic property behavior under tensile and compressive stress in steel," *IEEE Transactions on Magnetics*, vol. 33, no. 5, pp. 3958–3960, 1997.

[25] J. Li and M. Xu, "Modified jiles-atherton-sablik model for asymmetry in magnetomechanical effect under tensile and compressive stress," *Journal of Applied Physics*, vol. 110, no. 6, 2011.

[26] E. W. Lee, "Magnetostriction and magnetomechanical effects," *Reports on Progress in Physics*, vol. 18, no. 1, p. 184, 1955.

[27] M. Sablik, G. Burkhardt, H. Kwun, and D. Jiles, "A model for the effect of stress on the low-frequency harmonic content of the magnetic induction in ferromagnetic materials," *Journal of Applied Physics*, vol. 63, no. 8, pp. 3930–3932, 1988.

[28] M. J. Sablik and D. C. Jiles, "Coupled magnetoelastic theory of magnetic and magnetostrictive hysteresis," *IEEE Transactions on Magnetics*, vol. 29, no. 4, pp. 2113–2123, 1993.

[29] F. Liorzou and D. Atherton, "Effects of compressive stress on a steel cube using tensor magnetization and magnetostriction analysis," *Journal of Magnetism and Magnetic Materials*, vol. 195, no. 1, pp. 174–181, 1999.

[30] T. Yamasaki, S. Yamamoto, and M. Hirao, "Effect of applied stresses on magnetostriction of low carbon steel," *NDT & E International*, vol. 29, no. 5, pp. 263–268, 1996.

[31] O. Hubert, L. Daniel, and R. Billardon, "Experimental analysis of the magnetoelastic anisotropy of a non-oriented silicon iron alloy," *Journal of Magnetism and Magnetic Materials*, vol. 254, pp. 352–354, 2003.

[32] D. Jiles, "Theory of the magnetomechanical effect," *Journal of Applied Physics*, vol. 28, no. 8, p. 1537, 1995.

[33] P. Wilson, J. Ross, and A. Brown, "Optimizing the jiles-atherton model of hysteresis by a genetic algorithm," *IEEE Transactions on Magnetics*, vol. 37, no. 2, pp. 989–993, 2001.

[34] D. Miljavec and B. Zidari, "Introducing a domain flexing function in the jilesatherton hysteresis model," *Journal of Magnetism and Magnetic Materials*, vol. 320, no. 5, pp. 763 – 768, 2008.

[35] M. Toman, G. Stumberger, and D. Dolinar, "Parameter identification of the jiles-atherton hysteresis model using differential evolution," *IEEE Transactions on Magnetics*, vol. 44, no. 6, pp. 1098–1101, 2008.

[36] D. C. Jiles, J. Thoelke, and M. Devine, "Numerical determination of hysteresis parameters for the modeling of magnetic properties using the theory of ferromagnetic hysteresis," *IEEE Transactions on Magnetics*, vol. 28, no. 1, pp. 27–35, 1992.